SI-PET-RAFT: Surface-Initiated Photo-Induced Electron Transfer-Reversible Addition–Fragmentation Chain Transfer Polymerization

Mingxiao Li,[†] Michele Fromel,[†] Dhanesh Ranaweera,[†] Sergio Rocha,[†] Cyrille Boyer,[‡*] Christian W. Pester[†§*]

[†] Department of Chemical Engineering, The Pennsylvania State University, University Park, PA 16802, USA

[‡] School of Chemical Engineering, The University of New South Wales, UNSW Sydney NSW 2052, Australia

[§] Department of Materials Science and Engineering, The Pennsylvania State University, University Park, PA 16802, USA

ABSTRACT: In this communication, Surface-Initiated Photo-induced Electron Transfer-Reversible Addition–Fragmentation Chain Transfer Polymerization (SI-PET-RAFT) is introduced. SI-PET-RAFT affords functionalization of surfaces with spatiotemporal control and provides oxygen tolerance under ambient conditions. All hallmarks of controlled radical polymerization (CRP) are met, affording well-defined polymerization kinetics, and chain end retention to allow subsequent extension of active chain ends to form block copolymers. The modularity and versatility of SI-PET-RAFT is highlighted through significant flexibility with respect to the choice of monomer, light source and wavelength, and photoredox catalyst. The ability to obtain complex patterns in the presence of air is a significant contribution to help pave the way for CRP-based surface functionalization into commercial application.

The coating of surfaces with organic materials finds widespread use in our daily lives. For instance, polymeric coatings assure that eye glasses are easier to clean, that food does not stick to frying pans, and that displays are not charged with static electricity. Albeit powerful in their function, the physisorbed nature of many of these coatings inherently limits their advancement into new areas of research and application where precise topographical and/or chemical patterning is desirable or required.

Covalently surface-tethered macromolecules (polymer brushes) show great promise to address these limitations.[1–5] Various Surface-Initiated Controlled Radical Polymerization (SI-CRP) platforms provide access to thin polymer brush films with controllable thickness and chemical composition.[1] Surface-Initiated Nitroxide Mediated Polymerization (SI-NMP),[6,7] Atom Transfer Radical Polymerization (SI-ATRP),[8,9] and Reversible Addition-Fragmentation Chain-Transfer polymerization (SI-RAFT),[10] all provide powerful pathways towards versatile and patterned polymer surfaces with targeted functionalities. Potential areas of utilization include, but are not limited to, antifouling coatings,[11–14] drug delivery,[15] sensing,[16–20] catalysis,[21] as well as generally stimuli-responsive,[22–24] and opto-electronic materials.[25]

In addition to uniform coatings, recent scientific efforts have facilitated the fabrication of three-dimensionally patterned polymer brush surfaces.[26,27] Whereas previously most experimental techniques were often laborious, expensive, and limited to small substrates, the use of photoredox chemistry to catalyze polymerization has revolutionized the SI-CRP field.[28–30] The use of light in the visible wavelength region now provides a mild, eco-friendly, and non-invasive stimulus for selective polymer growth with spatiotemporal control and an elegant chemical and engineering tool to provide access to three-dimensional nanostructures.[26,27,31,32]

One significant challenge remains: SI-CRP's limited tolerance to ambient oxygen and chemical impurities is detrimental to the large-scale and commercial utilization of surface-tethered macromolecules. The presence of active oxygen species leads to considerable side reactions and chain termination events, limiting the ability to target well-defined polymer molecular weights with low dispersities. Aside complex strategies (e.g., addition of reducing agents),[8,33] there exist only a finite number of chemical systems which inherently mitigate the limitation of oxygen tolerance on surfaces and in SI-CRP.[31,34] For example, Diskekici et al. elaborated on a functionalized phenothiazine photoredox catalyst which indeed provided limited oxygen tolerance for polymerization and small molecule dehalogenation reactions.[31]

Here, these challenges are addressed by introducing oxygen tolerance into a SI-RAFT system. RAFT is an ideal platform with recent work suggesting that polymerization can be achieved in a broad range of solvents, even in whiskey.[35] The work outlined below draws inspiration from recent advances in Photoinduced Electron Transfer-Reversible Addition–Fragmentation Chain-Transfer (PET-RAFT) polymerization.[36,37] Significantly, PET-RAFT – in air and ambient conditions – can polymerize a large range of both less activated monomers (such as vinyl acetate) and more-activated monomers ((meth)acrylates, (meth)acrylamides) to afford macromolecules with well-defined structures and narrow dispersities under a broad range of visible wavelengths (from blue to near-infra-red light). The PET-RAFT mechanism involves visible-light-induced activation of either transition

metal-based (e.g., Tris(2-phenylpyridine)iridium(III) (*fac*-[Ir(ppy)$_3$]),[36] zinc tetraphenylporphyrin (ZnTPP),[37] and Ru(bpy)$_3$Cl$_2$)[38,39] or organic (e.g., Eosin Y)[40,41] photoredox catalysts and subsequent electron or energy transfer between the catalyst and the RAFT chain transfer agent (CTA) to mediate polymerization.

In the following, we will introduce *Surface-Initiated* PET-RAFT as a new synthetic platform for targeted surface functionalization. We will provide scientific evidence to confirm the hallmarks of CRP: The ability to target film thickness with well-defined kinetics and chain end fidelity. The ability to manufacture block copolymers and the utilization of light of various wavelengths in combination with photomasks will be highlighted to illustrate the ability to provide spatiotemporal control and access advanced 3D topographical and chemical patterns. Significantly, the following studies will emphasize the oxygen tolerance of SI-PET-RAFT by using ZnTPP as a photocatalyst. This eliminates the need for rigorous degassing or the work in inert atmospheres or with expensive equipment. We are convinced the benefits of our approach can help advance SI-CRP into academic and industrial application.

Figure 1a illustrates the concept of SI-PET-RAFT. A CTA-functionalized surface is irradiated uniformly under a given wavelength to grow surface-tethered macromolecules via a surface-initiated controlled radical polymerization. Subsequently, after thorough cleaning to remove any physisorbed polymers, variable angle spectroscopic ellipsometry (VASE) is used to determine the final polymer brush film thickness, *d*.

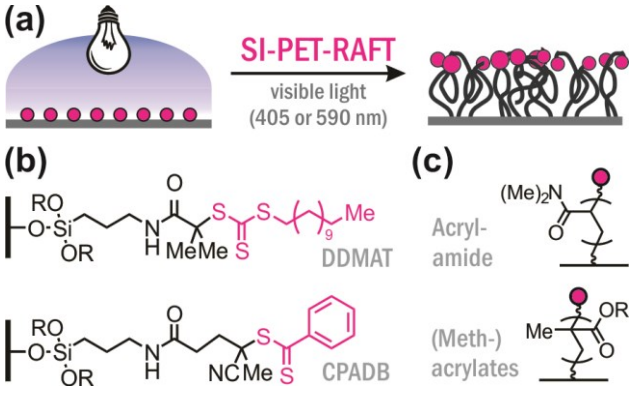

Figure 1. (a) Schematic of Surface-Initiated Photo-Induced Electron Transfer-Reversible Addition–Fragmentation Chain-Transfer Polymerization (SI-PET-RAFT). (b) Chemical structures of two different chain transfer agents (CTAs), DDMAT and CPADB, that were covalently immobilized on SiO_2 surfaces to allow growth of surface-initiated (c) acrylamide-, methacrylate-, and acrylate-based polymer brushes.

For surface functionalization, the Z-group approach was chosen, affording both a chemically robust attachment to the substrate as well as sequential monomer insertion into surface-tethered polymer chains without the entire macromolecule detaching and re-connecting to the surface.[1]

The reactivity of RAFT agents is dependent on both the Z and R group substituents.[42,43] Both dithio and trithio carbonate-based RAFT CTAs were synthesized and immobilized on silica surfaces to provide access to a wide range of monomers (see **Figure 1b**). X-ray photoelectron spectroscopy (XPS) confirmed covalent attachment of both 4-cyano-4-(phenylcarbonothioylthio)pentanoic acid (CPADB) as well as 2-(dodecylthiocarbonothioylthio)-2-methylpropionic acid (DDMAT) RAFT CTAs to SiO_2 via the presence of a nitrogen N1s peak at BE_{N1s} = 400 eV (see Supporting Information, Figure S3). Sulfur S2p (BE_{S2p} ≈ 164 eV) peaks of the CTA monolayer were prohibitively challenging to detect due to signal overlap with the pronounced Si2s peak of the underlying substrate. DDMAT and CPADB span the reactivity range to provide access to polymers comprised of acrylamides (former) and (meth)acrylates (latter, vide infra).[43,44]

Kinetic studies supported a controlled radical polymerization (CRP). In **Figure 2**, ZnTPP was used as a photocatalyst to mediate growth of *N*,*N*-dimethylacrylamide (DMA) polymer brushes on DDMAT-functionalized silica substrates. The rate of RAFT polymerization can be controlled both via the ratio of Monomer (M) to RAFT CTA and the concentration of photocatalyst (Photocat.), as well as the wavelength of irradiation. Optimized conditions for DMA, ZnTPP, and DDMAT were found at [M]:[CTA]:[Photocat] = 500:1:0.025 under irradiation with blue light (λ = 405 nm) (see Figure 2). Increasing the amount of free RAFT CTA ([M]:[RAFT CTA] = 200:1) and using yellow light (λ = 590 nm) decreased polymerization rates while however maintaining good control and high reproducibility of *d* vs. time.

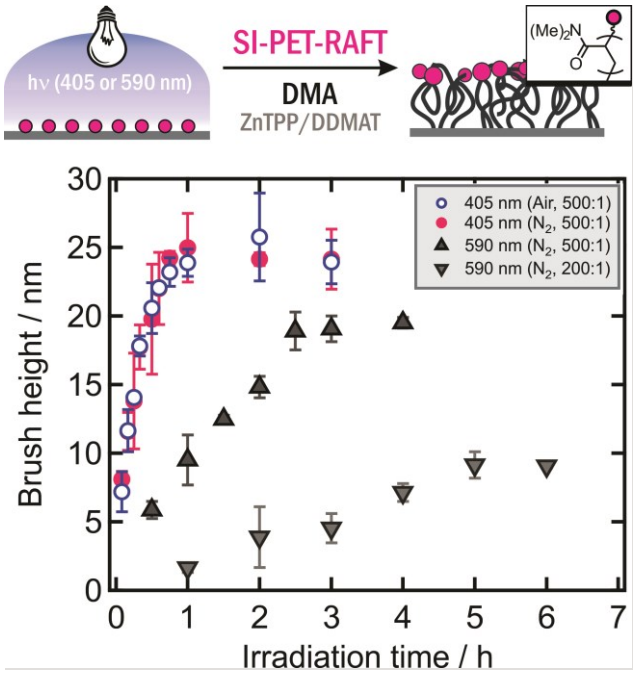

Figure 2. Polymer brush film thickness vs. irradiation time for SI-PET-RAFT of DMA using ZnTPP as the photocatalyst and DDMAT as the chain-transfer agent. Probing yellow (λ = 590 nm, triangles) and blue (λ = 405 nm, circles) irradiation wavelengths and monomer to chain transfer agent ratios (200:1 and 500:1 for yellow light, triangles), both in an inert nitrogen atmosphere (filled circles) as well as open to air (empty circles). Data suggests that controlled thickness is achievable irrespective of the presence of ambient oxygen.

Significantly, polymer brush rates fully open to air and in ambient conditions equal those in an inert nitrogen atmos-

phere glovebox (empty and filled circles in Figure 2, respectively). This oxygen tolerance poses significant advantages as it eliminates the time-consuming, rigorous deoxygenation step that is commonly required prior to conventional SI-CRP.

Mechanistically, the presence of free CTA in solution results in the growth of polymer not only at the surface, but also in solution. Boyer et al. have described first order kinetics for PET-RAFT in solution and a linear increase of $\ln([M]_0/[M]_t)$ with irradiation time.[45–47] For SI-PET-RAFT, the small microliter reagent volume that is used for polymerization from the surface makes purification and characterization of the free polymer that is formed in solution prohibitively challenging. Previous solution studies can therefore neither be supported nor rebutted.

Regarding the evolution of film thickness, d, vs. irradiation time, reports on SI-CRP are divided between first-order[48,49] or linear relationships.[13,27,31,32,50] For thermally-initiated SI-RAFT from flat substrates, scientific literature and kinetic data are more sparse, with no clear consensus emerging regarding the growth kinetics of surface-tethered brushes.[51–53] For optimized SI-PET-RAFT conditions (see **Figure 2**), polymer brush thickness, d, increases as a function of irradiation time, t, to provide access to thin films of up to $d_{p(DMA)}$ = 25 nm within an hour of 1.1 μW/cm² irradiation time at a rate of up to dd/dt = 25 nm hr^{-1}.

Control experiments show no polymer growth in the dark or in the absence of ZnTPP or any other photocatalyst we studied (see Supporting Information, Figure S4). In accordance with scientific literature on thermally-initiated SI-RAFT, experiments in the *absence* of free CTA in solution indicate that control over polymerization is lost (see Supporting Information, Figure S5).[51,54–56] 'Free' RAFT CTA benefits the efficient exchange reaction between graft and free polymers[55] and decreases the likelihood of radical-radical coupling reactions on the surface.[54] Without free CTA, rapid polymer growth leads to less uniform films with increased surface roughness. Chain extension experiments prove to be unsuccessful, indicating a loss of chain end functionality. These findings are coherent with what would be expected from an uncontrolled, surface-initiated free radical polymerization.

Simultaneous polymerization in solution (vide supra) implies limitations with respect to the maximum attainable film thickness (limited to $d \approx 25$ nm, see Figure 2). As the reaction proceeds, high molecular weight polymer is formed in the solution away from the substrate, thereby increasing solution viscosity and limiting further polymer brush growth by hindering RAFT CTA diffusion. To circumvent limitations imposed by increased viscosity of 'free' polymers, we leveraged a central characteristic of CRP: chain end retention (see **Figure 3**). After polymerizing an initial |-p(DMA) layer, the reaction is halted at low monomer conversion by switching off the light source. This first step allows to maintain a low solution viscosity while polymer brushes are grown. After washing the substrate of unreacted monomer and free polymer chains, a fresh solution of DMA monomer, ZnTPP, and DDMAT RAFT CTA is added anew, and the initial polymer brushes are extended. By repeating this step, it is possible to obtain |-p(DMA) polymer brush layers with thicknesses of up to d = 170 nm (see Figure 3). Consequently, sequential growth with individual polymerizations run to low conversions alleviates negative implications that the simultaneous growth of 'free' polymers in solution has on the ability to target specific polymer brush thicknesses on the surface.

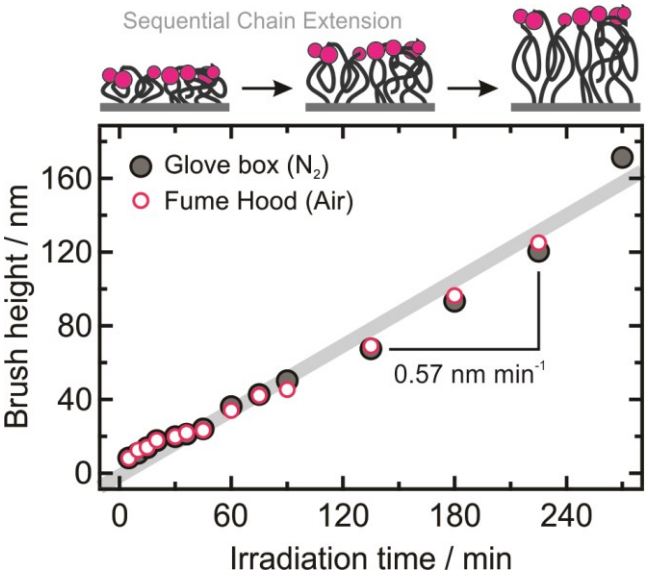

Figure 3. Polymer brush film thickness vs. irradiation time for the multi-step chain extension of |-p(DMA) brushes both in air (empty circles) and nitrogen atmosphere (filled circles) to achieve increased final film thickness. The gray line serves as a guide to the eye. Between each data point, the substrate was cleaned and a new solution of DMA, DDMAT, and ZnTPP was added.

Here, it is worth commenting on the kinetics: although Figure 2 indicates a first order behavior for SI-PET-RAFT, sequential extension suggests a linear relationship of thickness vs. time (see Figure 3). Individual polymerizations are carried out only to low conversions, possibly overshadowing the onset of decreased polymer chain growth kinetics at advanced stages of a first-order kinetic process. Excluding detrimental effects of highly viscous free polymers, control over thin film growth kinetics are improved. As indicated in Figure 3, polymer brush thickness increases linearly with time at a rate of dd/dt = 0.57 nm min^{-1}.

A profound advantage of SI-PET-RAFT is the ability to exert spatial control over polymerization kinetics through a difference of photon flux and perform topographical patterning. Utilizing this specific property, we decided to prepare 3D patterned surfaces (see **Figure 4a**). In contrast to conventional light-mediated SI-CRP techniques, which – aside a few exceptions[31] – require rigorous deoxygenation, SI-PET-RAFT patterning is possible under ambient conditions and in the presence of oxygen, thereby avoiding the use of advanced air-free Schlenk techniques or inert glove box environments.

Similarly to our previous work on reduction photolithography,[27] we used an array of optical lenses to project the pattern of a grayscale photomask image onto a CTA-functionalized substrate and perform SI-PET-RAFT of DMA under optimized conditions (see Supporting Information, Figure S9, for a schematic of the lithography setup). **Figure**

4b shows an optical micrograph of the resulting |-p(DMA) polymer brush reproduction of an original photograph (**Figure 4b** inset) of Sydney's Opera House and Harbor Bridge on a RAFT CTA-functionalized SiO_2 wafer. Optical contrast results from distinct heights of the polymer brushes in separate areas as a result of different levels of photon flux, i.e., light intensity. Using focal lengths of f_1 = 500 mm and f_2 = 100 mm, the features of the original photomask image are reproduced on the surface with a linear reduction of LRF = f_1/f_2 = 5, equaling a 25x reduction in area. Atomic Force Microscopy (AFM) confirmed the topographical complexity of the patterned substrate with high fidelity on the micron scale (see **Figure 4c**).

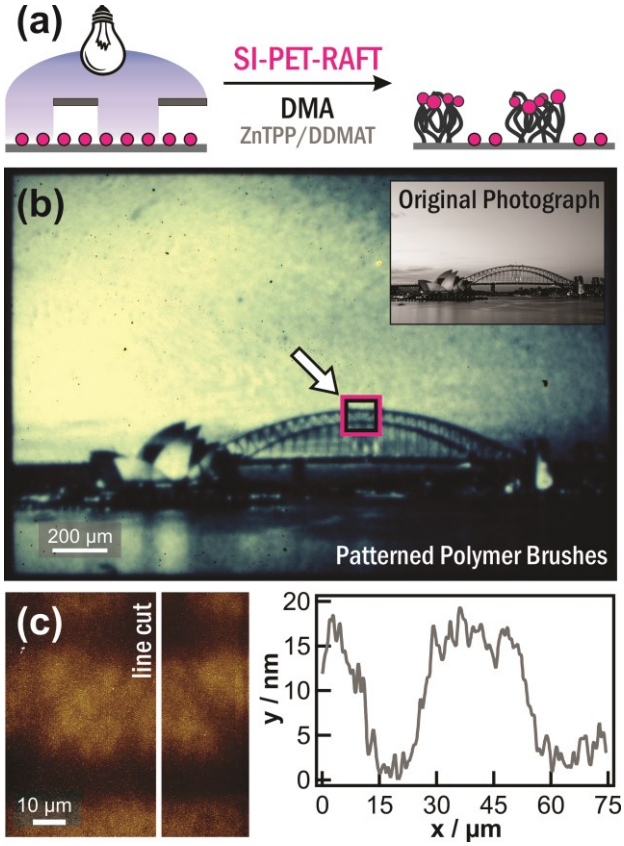

Figure 4. (a) Schematic of spatially controlled SI-PET-RAFT via localized irradiation of a CTA-functionalized substrate. (b) Optical micrograph of a |-p(DMA) (light) polymer brush reproduction of an original photomask (inset) on SiO_2 (dark) via a reduction photolithography process. (c) Atomic Force Micrograph at the location marked with a magenta box in (b) and corresponding line cut.

Despite the simultaneous growth of free bulk polymer in the reaction solution (vide supra), this is not detrimental to the ability of SI-PET-RAFT to pattern surfaces with high local resolution. The millisecond lifetimes of both RAFT CTA radicals and activated photocatalyst allows diffusion only on the order of nanometers.[37,57,58] This helps prevent a blurring-out of the projected photomask pattern and assures a spatially well-defined, micron-scale reproduction of the original photomask image.

In order to expand monomer tolerance and the scope of accessible polymers, CPADB was studied as another surface-tethered CTA (vide supra).[43,44] In combination with photocatalysts with stronger redox potentials, such as $Ir(ppy)_3$, these CPADB-functionalized surfaces help broaden the monomer scope that can be polymerized via the SI-PET-RAFT process. Successful SI-PET-RAFT was established for hydrophilic, hydrophobic, and functional (meth)acrylates, i.e., methyl methacrylate (MMA), 2,2,2-trifluoroethyl methacrylate (TFEMA), poly(ethylene glycol) methacrylate (PEGMA), and *N*-(methacryloxy)succinimide, as well as butyl acrylate (BuA) by using the ZnTPP/DDMAT combination (see Supporting Information).

Chain end retention and the ability to synthesize block copolymers is an important benefit of SI-CRP. Indeed, leveraging the expanded monomer scope, SI-PET-RAFT diblock copolymerization experiments suggest that the RAFT chain end is maintained throughout the initial polymerization step. Initial studies were targeted at sequential SI-PET-RAFT (see **Figure 5a-c**). After preparation of a poly(methyl methacrylate), |-p(MMA), homopolymer polymer brush, a diblock copolymer was synthesized via chain extension using 2,2,2-trifluoroethyl methacrylate (TFEMA) as the monomer. Ellipsometry confirmed an increase in film thickness from initially $d_{p(MMA)}$ = 19 nm for the |-p(MMA) homopolymer brush layer to $d_{p(MMA\text{-}b\text{-}TFEMA)}$ = 29 nm for the final |-p(MMA-*b*-TFEMA) diblock copolymer brush. A three- and four-layer model was used to fit the homopolymer and diblock copolymer thickness and optical constants, respectively (see Supporting Information, Figure S10). X-ray photoelectron spectroscopy (XPS) spectra for |-p(MMA) and |-p(MMA-*b*-TFEMA) are shown in **Figure 5b** and **c**, respectively. The emergence of a carbon signal at BE = 292.72 eV, attributed to $-\underline{C}F_3$, provided unambiguous evidence for growth of the second block (see **Figure 5c**). To illustrate the compatibility between SI-PET-RAFT and thermal SI-RAFT, an initial polystyrene (|-p(S)) homopolymer brush (d_{PS} = 31 nm) was grown via thermally-initiated SI-RAFT, using 2,2′-Azobis(2-methylpropionitrile) (AIBN) as the radical source and styrene (S) as monomer. The initial polymer brushes were then extended with DMA using SI-PET-RAFT to form a |-p(S-*b*-DMA) diblock copolymer brushes with a total film thickness of $d_{p(S\text{-}b\text{-}DMA)}$ = 54 nm (see **Figure 5d-f**). Again, XPS confirmed growth of the second block.

The combined ability to provide spatial control while retaining chain end functionality is essential for advanced and diverse patterning capabilities. **Figure 6** illustrates sequential SI-PET-RAFT polymerizations to fabricate complex topographies. First, a patterned |-p(DMA) homopolymer layer was prepared by using a striped photomask (see **Figure 6a**). After rinsing and cleaning the substrate, the photomask was rotated by 90° and a subsequent chain extension experiment was conducted, again using DMA as the monomer. A micrograph of the resulting crossed |-p(DMA-*b*-DMA) extended polymer cross-pattern is depicted in **Figure 6b**. Please note, native oxide SiO_2 wafers were used for these experiments, switching the optical contrast in the micrograph when compared to Figure 4. This experiment was conducted both in the presence of air (Figure 6) as well as under inert nitrogen conditions in a glove box (see Supporting Information, Figure S8). The results were indistinguishable from one another, supporting our findings that SI-PET-RAFT can be spatially controlled and allows re-initiation of chain ends in the presence of air and ambient conditions.

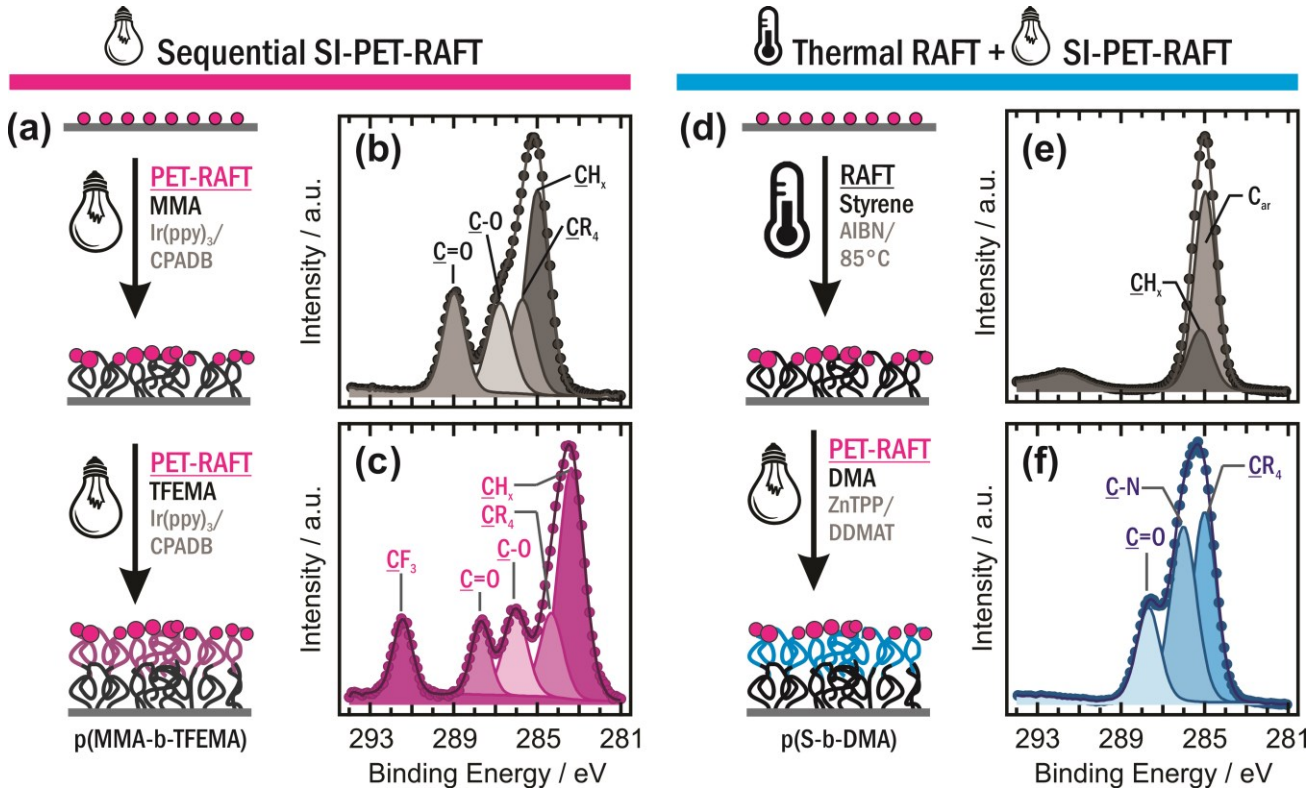

Figure 5. Diblock copolymers via SI-RAFT can be synthesized either via (a) two subsequent SI-PET-RAFT procedures or (d) a sequential combination of thermally-initiated SI-RAFT and SI-PET-RAFT. X-ray photoelectron spectra (XPS) confirmed growth of diblock copolymer brushes for (b) the initial p(MMA) and (c) final p(MMA-*b*-TFEMA) through emergence of a –CF_3 peak at 292.72 eV. Analogously, XPS was used to verify extension of (e) p(S) homopolymer brushes with p(DMA) to form (f) p(S-*b*-DMA) diblock copolymer brushes.

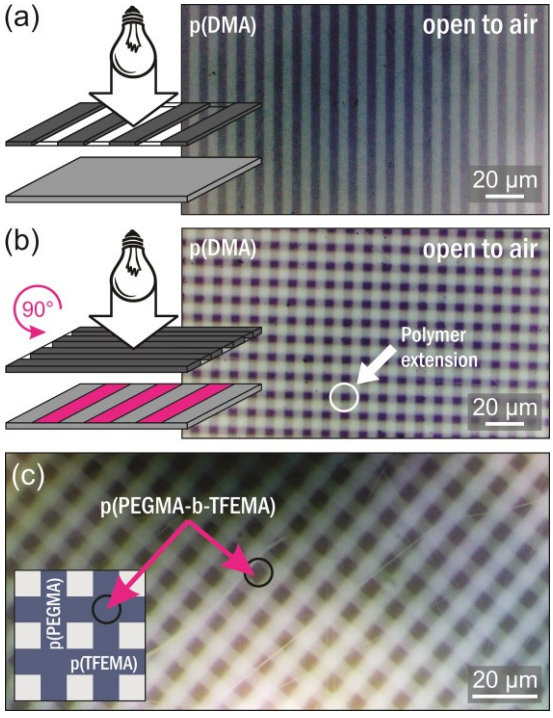

Figure 6. Sequential patterning of orthogonal stripes. (a) An initial layer of *N*,*N*-dimethylacrylamide was grown via SI-PET-RAFT using a striped photomask. The substrate was then cleaned and (b) a second SI-PET-RAFT polymerization was performed after rotating the striped photomask by 90 degrees. Optical micrographs confirmed chain extension and cross-patterning (circle) (c) The same experiment can be performed to grow cross-patterned PEGMA and TFEMA polymer brushes. In this case the intersection is comprised of a |-p(PEGMA-*b*-TFEMA) diblock copolymer.

In addition to this homopolymer extension, we also performed this experiment using two chemically disparate monomers. **Figure 6c** displays the result of cross-patterned p(PEGMA) and p(TFEMA) brushes grown from CPADB-functionalized substrates and using Ir(ppy)$_3$ as the photocatalyst. The highlighted intersections are now comprised of |-p(PEGMA-*b*-TFEMA) diblock copolymer brushes.

In conclusion, this contribution introduced the concept of light-mediated PET-RAFT to surface-initiated controlled radical polymerization. The SI-PET-RAFT platform provides a high degree of oxygen tolerance and allows controlled fabrication of uniform polymer brush layers, block copolymer brush layers, and sophisticated topographically and chemically patterned surfaces. Functionalized substrates are readily obtained and fully compatible with conventional, thermally-initiated SI-RAFT polymerization. A series of different photocatalysts and wavelengths were discussed and demonstrated, providing access to hydrophilic, hydrophobic, and functional polymer films. Although the simultaneous growth of polymer in the bulk reaction solution was found to prevent growth of very thick polymer films, this

limitation could be circumvented by sequential chain extension to yield thick films of d = 170 nm. Polymerization in solution did not negatively influence the ability for SI-PET-RAFT to provide access to well-defined topographically and chemically patterned surfaces. Ongoing work is targeted at enhancing pattern fidelity and broadening tolerance with respect to responsive monomers, solvent choice, and oxygen-tolerance for the fabrication of functional and (re-)programmable coatings.

ASSOCIATED CONTENT

Supporting Information. Supporting Information is available free of charge on the ACS Publications website and includes: Synthetic procedures for DDMAT and CPADB CTAs; Procedure to deposit RAFT-CTA on SiO_2 surfaces; General procedures for SI-PET-RAFT and thermal SI-RAFT; XPS and micrographs of monomer tolerance; Patterning of poly(butyl acrylate) brushes; Control experiments without free CTA; Description of ellipsometry models; Control experiments without photocatalyst; Crossed pattern micrographs in inert atmosphere; Reduction lithography setup.

AUTHOR INFORMATION

Corresponding Author

*pester@psu.edu and *cboyer@unsw.edu.au

ACKNOWLEDGMENT

This work was supported by start-up funds generously provided by the Pennsylvania State University. We would like to acknowledge the Penn State Materials Characterization Lab for assistance with the XPS measurements. We appreciate the help of Dr. Kaila M. Mattson for initial experiments and that of Tanner Mengle for AFM.

REFERENCES

(1) Zoppe, J. O.; Ataman, N. C.; Mocny, P.; Wang, J.; Moraes, J.; Klok, H. A. Surface-Initiated Controlled Radical Polymerization: State-of-the-Art, Opportunities, and Challenges in Surface and Interface Engineering with Polymer Brushes. *Chem. Rev.* **2017**, *117* (3), 1105–1318.

(2) Tomlinson, M. R.; Wu, T.; Efimenko, K.; Genzer, J. Gradient Polymer Brushes: Preparation and Applications. *Polym. Prepr.* **2003**, *44*, 468–469.

(3) Li, B.; Yu, B.; Ye, Q.; Zhou, F. Tapping the Potential of Polymer Brushes through Synthesis. *Acc. Chem. Res.* **2015**, *48*, 229–237.

(4) Chen, T.; Amin, I.; Jordan, R. Patterned Polymer Brushes. *Chem. Soc. Rev.* **2012**, *41* (8), 3280.

(5) Edmondson, S.; Osborne, V. L. V.; Huck, W. T. S. W. Polymer Brushes via Surface-Initiated Polymerizations. *Chem. Soc. Rev.* **2004**, *33* (1), 14–22.

(6) Hawker, C. J.; Bosman, A. W.; Harth, E. New Polymer Synthesis by Nitroxide Mediated Living Radical Polymerizations. *Chem. Rev.* **2001**, *101*, 3661–3688.

(7) Husseman, M.; Malmstrom, E. E.; McNamara, M.; Mate, M.; Mecerreyes, D.; Benoit, D. G.; Hedrick, J. L.; Mansky, P.; Huang, E.; Russell, T. P.; Hawker, C. J. Controlled Synthesis of Polymer Brushes by "Living" Free Radical Polymerization Techniques. *Macromolecules* **1999**, *32* (5), 1424–1431.

(8) Matyjaszewski, K.; Hongchen, D.; Jakubowski, W.; Pietrasik, J.; Kusumo, A. Grafting from Surfaces for "Everyone": ARGET ATRP in the Presence of Air. *Langmuir* **2007**, *23* (8), 4528–4531.

(9) Liu, T.; Jia, S.; Kowalewski, T.; Matyjaszewski, K.; Casado-Portilla, R.; Belmont, J. Grafting Poly (n-Butyl Acrylate) from a Functionalized Carbon Black Surface by Atom Transfer Radical Polymerization. *Langmuir* **2003**, *19* (16), 6342–6345.

(10) *Surface-Initiated Polymerization I*; Jordan, R., Ed.; Springer-Verlag Berlin Heidelberg, 2006.

(11) Fan, X.; Lin, L.; Messersmith, P. B. Cell Fouling Resistance of Polymer Brushes Grafted from Ti Substrates by Surface-Initiated Polymerization: Effect of Ethylene Glycol Side Chain Length. *Biomacromolecules* **2006**, *7* (8), 2443–2448.

(12) Moroni, L.; Klein Gunnewiek, M.; Benetti, E. M. Polymer Brush Coatings Regulating Cell Behavior: Passive Interfaces Turn into Active. *Acta Biomater.* **2014**, *10* (6), 2367–2378.

(13) Pester, C. W.; Poelma, J. E.; Narupai, B.; Patel, S. N.; Su, G. M.; Mates, T. E.; Luo, Y.; Ober, C. K.; Hawker, C. J.; Kramer, E. J. Ambiguous Anti-Fouling Surfaces: Facile Synthesis by Light-Mediated Radical Polymerization. *J. Polym. Sci. Part A Polym. Chem.* **2016**, *54*, 253–262.

(14) Yang, W. J.; Neoh, K.-G.; Kang, E.-T.; Teo, S. L.-M.; Rittschof, D. Polymer Brush Coatings for Combating Marine Biofouling. *Prog. Polym. Sci.* **2014**, *39* (5), 1017–1042.

(15) Krishnamoorthy, M.; Hakobyan, S.; Ramstedt, M.; Gautrot, J. E. Surface-Initiated Polymer Brushes in the Biomedical Field: Applications in Membrane Science, Biosensing, Cell Culture, Regenerative Medicine and Antibacterial Coatings. *Chem. Rev.* **2014**, *114* (21), 10976–11026.

(16) Schüwer, N. B. Synthesis of Responsive Polymer Brushes for Sensing Applications, Ecole Polytechnique Federale de Lausanne, Suisse, 2011, Vol. 5077.

(17) Schüwer, N.; Klok, H. A. A Potassium-Selective Quartz Crystal Microbalance Sensor Based on Crown-Ether Functionalized Polymer Brushes. *Adv. Mater.* **2010**, *22* (30), 3251–3255.

(18) Schüwer, N.; Tercier-Waeber, M.-L.; Danial, M.; Klok, H.-A. Voltammetric Detection of Hg2+ Using Peptide-Functionalized Polymer Brushes. *Aust. J. Chem.* **2012**, *65*, 1104–1109.

(19) Bilgic, T.; Klok, H.-A. Surface-Initiated Controlled Radical Polymerization Enhanced DNA Biosensing. *Eur. Polym. J.* **2015**, *62*, 281–293.

(20) Barbey, R.; Kauffmann, E.; Ehrat, M.; Klok, H. Protein Microarrays Based on Polymer Brushes Prepared via Surface-Initiated Atom Transfer Radical Polymerization. **2010**, 3467–3479.

(21) Koenig, M.; Magerl, D.; Philipp, M.; Eichhorn, K.-J.; Müller, M.; Müller-Buschbaum, P.; Stamm, M.; Uhlmann, P. Nanocomposite Coatings with Stimuli-Responsive Catalytic Activity. *RSC Adv.* **2014**, *4* (34), 17579–17586.

(22) Mazurowski, M.; Gallei, M.; Li, J.; Didzoleit, H.; Stühn, B.; Rehahn, M. Redox-Responsive Polymer Brushes Grafted from Polystyrene Nanoparticles by Means of Surface Initiated Atom Transfer Radical Polymerization. *Macromolecules* **2012**, *45* (22), 8970–8981.

(23) Rauch, S.; Uhlmann, P.; Eichhorn, K.-J. In Situ Spectroscopic Ellipsometry of PH-Responsive Polymer Brushes on Gold Substrates. *Anal. Bioanal. Chem.* **2013**, *405* (28), 9061–9069.

(24) Li, L.; Zhu, Y.; Li, B.; Gao, C. Fabrication of Thermoresponsive Polymer Gradients for Study of Cell Adhesion and Detachment. *Langmuir* **2008**, *24* (23), 13632–13639.

(25) Page, Z. A.; Narupai, B.; Pester, C. W.; Bou Zerdan, R.; Sokolov, A.; Laitar, D. S.; Mukhopadhyay, S.; Sprague, S.; McGrath, A. J.; Kramer, J. W.; Trefonas, P. Hawker, C. J. Novel Strategy for Photopatterning Emissive Polymer Brushes for Organic Light Emitting Diode Applications. *ACS Cent. Sci.* **2017**, *3* (6).

(26) Poelma, J. E.; Fors, B. P.; Meyers, G. F.; Kramer, J. W.; Hawker, C. J. Fabrication of Complex Three-Dimensional Polymer Brush Nanostructures through Light-Mediated Living Radical Polymerization. *Angew. Chemie-International Ed.* **2013**, *52* (27), 6844–6848.

(27) Pester, C. W.; Narupai, B.; Mattson, K. M.; Bothman, D. P.; Klinger, D.; Lee, K. W.; Discekici, E. H.; Hawker, C. J. Engineering Surfaces through Sequential Stop-Flow Photopatterning. *Adv. Mater.* **2016**, *28* (42).

(28) Pan, X.; Tasdelen, M. A.; Laun, J.; Junkers, T.; Yagci, Y.; Matyjaszewski, K. Photomediated Controlled Radical Polymerization. *Prog. Polym. Sci.* **2016**.

(29) Leibfarth, F. A.; Mattson, K. M.; Fors, B. P.; Collins, H. A.; Hawker, C. J. External Regulation of Controlled

Polymerizations. *Angew. Chemie-International Ed.* **2013**, *52* (1), 199–210.

(30) Fors, B. P.; Hawker, C. J. Control of a Living Radical Polymerization of Methacrylates by Light. *Angew. Chemie-International Ed.* **2012**, *51* (35), 8850–8853.

(31) Discekici, E. H.; Pester, C. W.; Treat, N. J.; Lawrence, J.; Mattson, K. M.; Narupai, B.; Toumayan, E. P.; Luo, Y.; McGrath, A. J.; Clark, P. G.; Read de Alaniz, J.; Hawker, C. J. Simple Benchtop Approach to Polymer Brush Nanostructures Using Visible-Light-Mediated Metal-Free Atom Transfer Radical Polymerization. *ACS Macro Lett.* **2016**, *5*, 258–262.

(32) Narupai, B.; Poelma, J. E.; Pester, C. W.; McGrath, A. J.; Toumayan, E. P.; Luo, Y.; Kramer, J. W.; Clark, P. G.; Ray, P. C.; Hawker, C. J. Hierarchical Comb Brush Architectures via Sequential Light-Mediated Controlled Radical Polymerizations. *J. Polym. Sci. Part A Polym. Chem.* **2016**, *54* (15).

(33) Ligon, S. C.; Husár, B.; Wutzel, H.; Holman, R.; Liska, R. Strategies to Reduce Oxygen Inhibition in Photoinduced Polymerization. *Chem. Rev.* **2014**, *114* (1), 577–589.

(34) Discekici, E. H.; Treat, N. J.; Poelma, S. O.; Mattson, K. M.; Hudson, Z. M.; Luo, Y.; Hawker, C. J.; de Alaniz, J. R. A Highly Reducing Metal-Free Photoredox Catalyst: Design and Application in Radical Dehalogenations. *Chem. Commun.* **2015**, *51* (58), 11705–11708.

(35) Schneiderman, D. K.; Ting, M.; Purchel, A. A.; Miranda, R.; Tirrell, M. V; Reineke, T. M.; Rowan, S. J. Open-to-Air RAFT Polymerization in Complex Solvents: From Whisky to Fermentation Broth. *ACS Macro Lett.* **2018**, *7*, 406–411.

(36) Xu, J.; Jung, K.; Atme, A.; Shanmugam, S.; Boyer, C. A Robust and Versatile Photoinduced Living Polymerization of Conjugated and Unconjugated Monomers and Its Oxygen Tolerance. *J. Am. Chem. Soc.* **2014**, *136* (14), 5508–5519.

(37) Shanmugam, S.; Xu, J.; Boyer, C. Exploiting Metalloporphyrins for Selective Living Radical Polymerization Tunable over Visible Wavelengths. *J. Am. Chem. Soc.* **2015**, *137* (28), 9174–9185.

(38) Xu, J.; Jung, K.; Corrigan, N. A.; Boyer, C. Aqueous Photoinduced Living/Controlled Polymerization: Tailoring for Bioconjugation. *Chem. Sci.* **2014**, *5* (9), 3568.

(39) Niu, J.; Page, Z. A.; Dolinski, N. D.; Anastasaki, A.; Hsueh, A. T.; Soh, H. T.; Hawker, C. J. Rapid Visible Light-Mediated Controlled Aqueous Polymerization with in Situ Monitoring. *ACS Macro Lett.* **2017**, *6* (10), 1109–1113.

(40) Figg, C. A.; Hickman, J. D.; Scheutz, G. M.; Shanmugam, S.; Carmean, R. N.; Tucker, B. S.; Boyer, C.; Sumerlin, B. S. Color-Coding Visible Light Polymerizations to Elucidate the Activation of Trithiocarbonates Using Eosin Y. *Macromolecules* **2018**, *51* (4), 1370–1376.

(41) Watanabe, A.; Niu, J.; Lunn, D. J.; Lawrence, J.; Knight, A. S.; Zhang, M.; Hawker, C. J. PET-RAFT as a Facile Strategy for Preparing Functional Lipid–polymer Conjugates. *J. Polym. Sci. Part A Polym. Chem.* **2018**, *56* (12), 1259–1268.

(42) Mayadunne, R. T. A.; Rizzardo, E.; Chiefari, J.; Krstina, J.; Moad, G.; Postma, A.; Thang, S. H. Living Polymers by the Use of Trithiocarbonates as Reversible Addition-Fragmentation Chain Transfer (RAFT) Agents: ABA Triblock Copolymers by Radical Polymerization in Two Steps. *Macromolecules* **2000**, *33* (2), 243–245.

(43) Chiefari, J.; Chong, Y. K. B.; Ercole, F.; Krstina, J.; Jeffery, J.; Le, T. P. T.; Mayadunne, R. T. A.; Meijs, G. F.; Moad, C. L.; Moad, G.; Rizzaro, E.; Thang, S. H. Living Free-Radical Polymerization by Reversible Addition−Fragmentation Chain Transfer: The RAFT Process. *Macromolecules* **1998**, *31* (98), 5559–5562.

(44) Perrier, S. 50th Anniversary Perspective : RAFT Polymerization - A User Guide. *Macromolecules* **2017**, *50*, 7433–7447.

(45) Shanmugam, S.; Xu, J.; Boyer, C. Photoinduced Electron Transfer-Reversible Addition-Fragmentation Chain Transfer (PET-RAFT) Polymerization of Vinyl Acetate and N-Vinylpyrrolidinone: Kinetic and Oxygen Tolerance Study. *Macromolecules* **2014**, *47* (15), 4930–4942.

(46) Ng, G.; Yeow, J.; Chapman, R.; Isahak, N.; Wolvetang, E.; Cooper-white, J. J.; Boyer, C. Pushing the Limits of High Throughput PET-RAFT Polymerization. *Macromolecules* **2018**, *51*, 7600–7607.

(47) Xu, J.; Jung, K.; Boyer, C. Oxygen Tolerance Study of Photoinduced Electron Transfer–Reversible Addition–Fragmentation Chain Transfer (PET-RAFT) Polymerization Mediated by $Ru(Bpy)_3Cl_2$. *Macromolecules* **2014**, *47* (13), 4217–4229.

(48) Vorobii, M.; Pop-Georgievski, O.; De Los Santos Pereira, A.; Kostina, N. Y.; Jezorek, R.; Sedlakova, Z.; Percec, V.; Rodriguez-Emmenegger, C. Grafting of Functional Methacrylate Polymer Brushes by Photoinduced SET-LRP. *Polym. Chem.* **2016**, *7*, 6934–6945.

(49) Sumerlin, B. S.; Neugebauer, D.; Matyjaszewski, K. Initiation Efficiency in the Synthesis of Molecular Brushes by Grafting from via Atom Transfer Radical Polymerization. *Macromolecules* **2005**, *38*, 702–708.

(50) Poelma, J. E.; Fors, B. P.; Meyers, G. F.; Kramer, J. W.; Hawker, C. J. Fabrication of Complex Three-Dimensional Polymer Brush Nanostructures through Light-Mediated Living Radical Polymerization - SUPPLEMENT. *Angew. Chemie-International Ed.* **2013**, *52*, 6844 –6848.

(51) Baum, M.; Brittain, W. J. Synthesis of Polymer Brushes on Silicate Substrates via Reversible Addition Fragmentation Chain Transfer Technique. *Macromolecules* **2002**, *35* (3), 610–615.

(52) Demirci, S.; Kinali-Demirci, S.; Caykara, T. A New Selenium-Based RAFT Agent for Surface-Initiated RAFT Polymerization of 4-Vinylpyridine. *Polym. (United Kingdom)* **2013**, *54* (20), 5345–5350.

(53) Kitano, H.; Liu, Y.; Tokuwa, K. I.; Li, L.; Iwanaga, S.; Nakamura, M.; Kanayama, N.; Ohno, K.; Saruwatari, Y. Polymer Brush with Pendent Glucosylurea Groups Constructed on a Glass Substrate by RAFT Polymerization. *Eur. Polym. J.* **2012**, *48* (11), 1875–1882.

(54) Rowe, M. D.; Hammer, B. A. G.; Boyes, S. G. Synthesis of Surface-Initiated Stimuli-Responsive Diblock Copolymer Brushes Utilizing a Combination of ATRP and RAFT Polymerization Techniques. *Macromolecules* **2008**, *41* (12), 4147–4157.

(55) Ohno, K.; Ma, Y.; Huang, Y.; Mori, C.; Yahata, Y.; Tsujii, Y.; Maschmeyer, T.; Moraes, J.; Perrier, S. Surface-Initiated Reversible Addition-Fragmentation Chain Transfer (RAFT) Polymerization from Fine Particles Functionalized with Trithiocarbonates. *Macromolecules* **2011**, *44* (22), 8944–8953.

(56) Tsujii, Y.; Ejaz, M.; Sato, K.; Goto, A.; Fukuda, T. Mechanism and Kinetics of RAFT-Mediated Graft Polymerization of Styrene on a Solid Surface. 1. Experimental Evidence of Surface Radical Migration. *Macromolecules* **2001**, *34* (26), 8872–8878.

(57) Barner-Kowollik, C.; Russell, G. T. Chain-Length-Dependent Termination in Radical Polymerization: Subtle Revolution in Tackling a Long-Standing Challenge. *Prog. Polym. Sci.* **2009**, *34* (11), 1211–1259.

(58) Feldermann, A.; Coote, M. L.; Stenzel, M. H.; Davis, T. P.; Barner-Kowollik, C. Consistent Experimental and Theoretical Evidence for Long-Lived Intermediate Radicals in Living Free Radical Polymerization. *J. Am. Chem. Soc.* **2004**, *126* (48), 15915–15923.

TOC graphic – Table of Contents only